RSC Advances

PAPER

View Article Online
View Journal | View Issue

Cite this: *RSC Adv.*, 2019, **9**, 2116

Fabrication of graphite/MgO-reinforced poly(vinyl chloride) composites by mechanical activation with enhanced thermal properties

Qinghua Li,[a] Fang Shen,*[ab] Jingqi Ji,[a] Yanjuan Zhang,[a] Yaseen Muhammad,[bc] Zuqiang Huang,[a] Huayu Hu,*[a] Yunpeng Zhu[a] and Yuben Qin[a]

Received 14th November 2018
Accepted 20th December 2018

DOI: 10.1039/c8ra09384a

rsc.li/rsc-advances

In this study, a mechanical activation (MA) approach was developed to fabricate graphite/MgO-reinforced poly(vinyl chloride) (PVC) composites with superior thermal properties. The composites were characterized by scanning electron microscopy (SEM), differential scanning calorimetry (DSC), thermogravimetric analysis (TGA) and differential thermogravimetric (DTG) analysis. SEM results revealed uniformly dispersed graphite and MgO flakes in a PVC matrix and the successful formation of a thermal network by MA, which led to enhanced thermal conductivity. DSC and TGA results of the composites showed enhancement in the glass transition temperature (Tg) from 82.81 °C to 88.60 °C and decomposition temperature from 287.61 °C to 305.59 °C as compared to pristine PVC. The thermal conductivity of the graphite/MgO/PVC composite at optimum conditions was 0.8791 W m^{-1} K^{-1}, which was 6.27 times higher than that of pristine PVC. The mechanical properties such as the tensile strength and bending strength of graphite/MgO/PVC composites were also augmented as compared to pristine PVC, graphite/PVC and MgO/PVC composites. Due to the enhanced thermal properties of the newly designed graphite/MgO/PVC composites, they have potential as alternatives to classical PVC-based materials in thermal and many other target field-based applications.

1. Introduction

The development of thermally conductive polymer composites containing nano-sized fillers, such as carbon black, metal and ceramic *etc.*, has attracted significant scientific attention recently. These conductive fillers grant improved thermal conductivity to polymers.[1–4] In this regard, metal-based materials due to their high thermal conductivity have extensively been applied. However, due to the poor insulation and low resistance to chemical corrosion, such applications are limited in areas such as electronic packaging, heat exchangers, chemical production, integrated circuits, and solar water heaters.[1,2,5] Among the conducting fillers, graphite has attracted significant attention due to its high electrical and thermal conductivity, chemical stability, facile and simplified synthesis, low cost, large surface area/volume ratio, and ease of processing into host polymers.[2,6–10] Apart from graphite, magnesium oxide (MgO) has also been used as an effective additive for thermally conductive polymers due to its cost effectiveness, wide range of available sources and large filling capacity.[11,12] Therefore, it is worth studying the integrated effect of graphite and MgO as additives on the thermal performance of conductive polymers.

Poly(vinyl chloride) (PVC), as a widely used polymer and one of the largest resin productions, has been applied in flooring materials, cable sheaths and construction pipes due to its low cost, good fire-retardancy and excellent resistance to corrosion.[13–16] However, its poor thermal conductivity (0.014 W m^{-1} K^{-1}) is a major disadvantage that hinders the widespread applications of PVC.[17,18] If a PVC-based material is modified by filling with thermally conductive agents that replace the expensive metals, it would concomitantly enhance the cost effectiveness and broaden the spectrum of applications for PVC to areas like heat transfer, electronic packaging, and architectural coverings.[2]

Traditional methods for improving the thermal properties of conductive polymer composites include *in situ* polymerization,[19] solution blending[20] and melt-mixing.[21] Chen *et al.*[19] reported high thermal conductivity polyamide-6 composites *via in situ* polymerization using small amounts of graphene oxide (GO)-stabilized graphene dispersions. He *et al.*[20] fabricated novel exfoliated graphite nanoplates/syndiotactic polystyrene composites with high thermal conductivity using solution-blending method. Yousefzade *et al.*[21] prepared nanocomposites based on ethylene-vinyl acetate copolymer and expanded graphite using melt-mixing approach. However, the

[a]School of Chemistry and Chemical Engineering, Guangxi University, Nanning 530004, China. E-mail: fangshen@gxu.edu.cn; yuhuahu@163.com; Fax: +86-771-3233718; Tel: +86-771-3233718

[b]Guangxi Key Laboratory of Petrochemical Resource Processing and Process Intensification Technology, Guangxi University, Nanning 530004, China

[c]Institute of Chemical Sciences, University of Peshawar, 25120, KP, Pakistan

earlier two methods are considered environmentally-unfriendly and complicated with convoluted steps. On the contrary, melt-mixing is simple and easy in operation, but faces problems of discharging dioxins and chlorine gas to the environment. In comparison to these approaches, the mechanical activation (MA) approach utilizes high-energy ball milling and is considered to be environmentally friendly, with simplified mechanization without the application of hazardous solvents.[22–24] The ball milling, shearing and friction in MA collectively decrease the particle size of the composites and results in a uniform dispersion of the filler in the polymer matrix. These factors cumulatively contribute to the cost effectiveness and environmental friendliness of the MA and hence can be applied as an efficient alternative approach for the preparation of thermally conductive materials.

Due to the importance of uniform dispersion of fillers in PVC-based composites, in the current work, graphite and MgO were applied as fillers and graphite/MgO/PVC composites were prepared by MA. Microstructural characterization of the resulting composites was performed by scanning electron microscopy (SEM), thermogravimetric analysis (TGA), and differential scanning calorimetry (DSC). Apart from this, mechanical properties like the tensile strength and bending strength and the effect of various factors *i.e.* graphite/MgO content, milling speed, and milling time on these properties, were systematically investigated.

2. Materials and methods

2.1. Materials

Flake graphite (99.9%) was supplied by Aladdin industrial corporation, Nanqiao Town, Feng xian, Shanghai, China. PVC (S65 type, *k*-value: 64.6–66.0, 0.12–0.14 W m^{-1} K^{-1}) was purchased from Formosa plastics industry (Ningbo) Co. Ltd (China). MgO and Glycerol were provided by Sinopharm Co, Ltd. (China). All chemical used were of analytical grade and used without further processing.

2.2. Preparation of graphite/MgO/PVC composites

Graphite/MgO/PVC composites were prepared from graphite, MgO and PVC *via* MA, as shown in Fig. 1. After reacting for a certain time under a constant bath temperature of 50 °C and aggressive ZrO_2 ball milling, the mixed powder was put into a mold which was smeared with lubricant (Glycerol). Finally, the mixed powder was pressed into the graphite/MgO/PVC composite material with a vulcanizing machine at 160 °C and 5 MPa for 15 min.

2.3. Characterization of composites

2.3.1. Thermal conductivity measurement. The thermal conductivity of graphite/MgO/PVC composites was measured by a thermal analyzer (Nanjing Dazhan research institute) in a range of 0.005–10 W m^{-1} K^{-1} with an accuracy of ≤±3%.

2.3.2. SEM analysis. The surface morphology analysis of the tensile fractured samples sprayed with gold were undertaken using an SEM (Hitachi S-3400N, Japan) at an operating voltage of 20 kV.

2.3.3. DSC analysis. DSC analysis of the composites was performed by a Q20 DSC analyzer (TA Instruments, USA) in the temperature range of −10–250 °C at a rate of 20 °C min^{-1} under an N_2 flow rate of 30 mL min^{-1}.

2.3.4. TGA analysis. TGA of the composites was carried out with a Q50 thermogravimetric analyzer (TA Instruments, USA) using a test sample of 10 mg over a temperature range of 30–600 °C at a heating rate of 20 °C min^{-1} under an N_2 flow rate of 30 mL min^{-1}.

2.3.5. Mechanical properties testing. The mechanical properties of the composites were measured with a MWW-20A

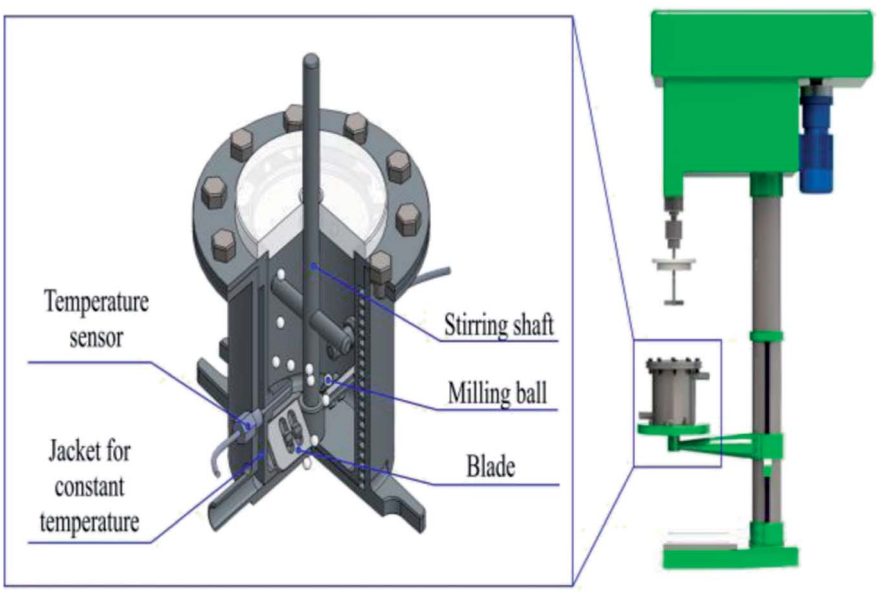

Fig. 1 Representation of stirring ball mill.

microcomputer control wood-based panel universal testing machine (Jinan Tianchen Testing Machine Manufacturing Co., Ltd, China). The tensile strength and elongation to breakage of the composites were measured at a crosshead speed of 2.0 mm min^{-1} in accordance with GB/T1040-92 (China) at room temperature.[25] Similarly, the bending strength was measured by a three-point bending tester at a crosshead speed of 1.0 mm min^{-1} according to GB/T9341-2000 (China) at room temperature.[25] All the experiments were performed five times and average values were reported.

3. Results and discussion

3.1. Effect of milling speed on thermal conductivity of graphite/MgO/PVC

Ball milling speed during MA has a marked effect on the properties of the composites.[26] The effect of the ball milling speed in Fig. 2 suggests that the thermal conductivity of the graphite/MgO/PVC composite increased with increments of the milling speed and reached maximum (0.8105 W m^{-1} K^{-1}) at 150 r per min. This could be attributed to the uniform distribution of the graphite in the PVC matrix resulting in a stronger thermal network structure. Upon increasing the milling speed beyond 150 r per min, the thermal conductivity decreased. At a milling speed exceeding a certain value, the solid-phase reaction tangential force of the ball milling was too large with high energy of collision among the molecules, causing the decomposition of a certain portion of the PVC,[27,28] resulting in sinking and uneven mixing. In such a scenario, the graphite would not uniformly mix with PVC, which led to increased thermal resistance and ultimately lower thermal conductivity. In addition, under high energy ball milling, some of the decomposition products of PVC and MgO could produce magnesium chloride which upon mixing with the composite sheet led to decreased thermal conductivity.[29,30] Based on the results in Fig. 2, an optimum milling speed of 150 r per min was applied for the subsequent experiments.

3.2. Effect of milling time on thermal conductivity of graphite/MgO/PVC

The reaction time during MA greatly affects the thermal properties of the composites.[22,23,31] The results compiled in Fig. 3 suggest that the thermal conductivity increased with increasing milling time from 0–60 min, which could be attributed to better contact between the composite particles at longer reaction times. This led to a uniform distribution of the fillers in the PVC matrix forming a stronger network structure and hence led to increased thermal conductivity. By Increasing the milling time beyond 60 min, the thermal conductivity of the composites decreased due to partial decomposition of the PVC which in turn reacted with MgO and formed magnesium chloride that had poor thermal conductivity.[29,30] This phenomenon got more severe with increasing time and hence the decrease in thermal conductivity continued to correspondingly increase. Considering the maximum thermal conductivity (Fig. 3) and energy consumption during operation, 60 min was chosen as the optimum milling time for the subsequent experiments.

3.3. Effect of graphite content on thermal conductivity of graphite/MgO/PVC

The thermal conductivity of the filled composite is greatly affected by the number of thermally conductive channels or networks formed and the effective packing rate of the conductive filler.[2,32] The results compiling the effect of graphite content on the thermal conductivity of graphite/MgO/PVC shown in Fig. 4 indicated a direct relation between the two parameters. As the thermal conductivity of MgO is lower than that of graphite, thus the conductivity of the composite was mainly controlled by the graphite conduction network, which was favored at higher graphite contents. From Fig. 4, at 20 wt% graphite loading, the maximum thermal conductivity of 0.7022 W m^{-1} K^{-1} was recorded. However, further increasing the graphite contents (up to 25 wt%) did not affect thermal conductivity. The main reason

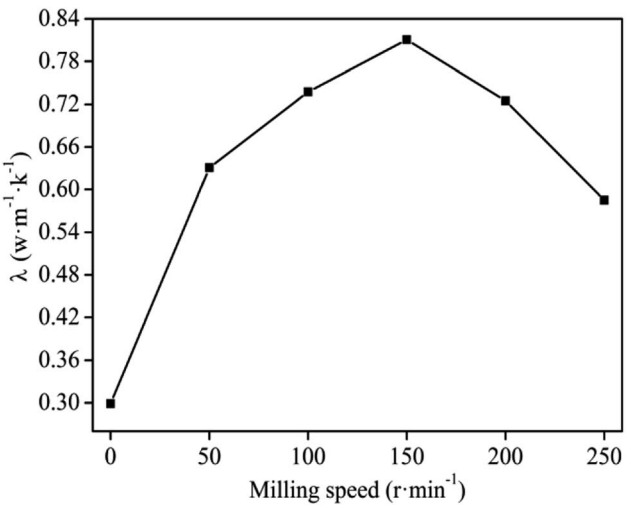

Fig. 2 Effect of milling speed on the thermal conductivity of graphite/MgO/PVC composite under MgO and graphite loadings of 10 wt% and 20 wt% respectively for 40 min milling.

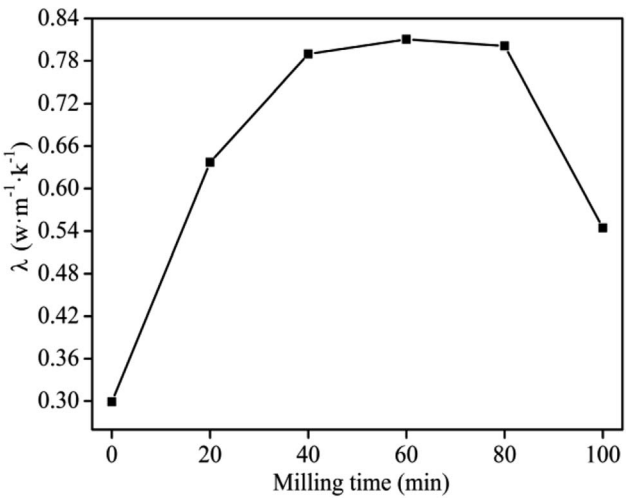

Fig. 3 Effect of milling time on thermal conductivity of graphite/MgO/PVC under a milling speed of 150 r per min, MgO and graphite contents of 10 wt% and 20 wt%, respectively.

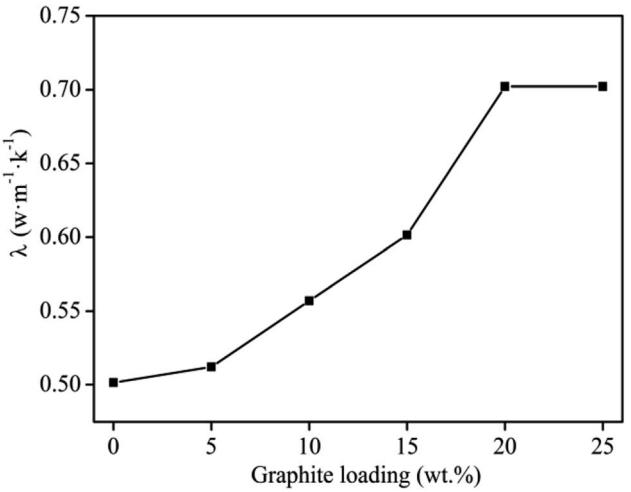

Fig. 4 Effect of graphite content on thermal conductivity of graphite/MgO/PVC at MgO loadings of 20 wt%, mill speed of 150 r per min and milling time of 60 min.

was that at 20 wt% graphite loading, the thermal network chains were uniformly formed throughout the matrix, and thermal conductivity of the composites reached to maximum (percolation threshold). Therefore, the optimum graphite content of 20 wt% was chosen for subsequent experiments.

3.4. Effect of MgO content on thermal conductivity of graphite/MgO/PVC

MgO is a thermally conductive filler with heat resistant and flame-retardant properties,[11,12] and thus its content greatly affects the thermal conductivity of the materials. At 150 r per min, 60 min milling time and a graphite content of 20 wt%, the effect of MgO content on thermal conductivity was investigated and plotted in Fig. 5. It can be seen that thermal conductivity directly increased with increasing MgO content in a range of 5–15 wt%, while achieving maximum (0.8791 W m^{-1} K^{-1}) at 15 wt%. The decrease in thermal conductivity on further

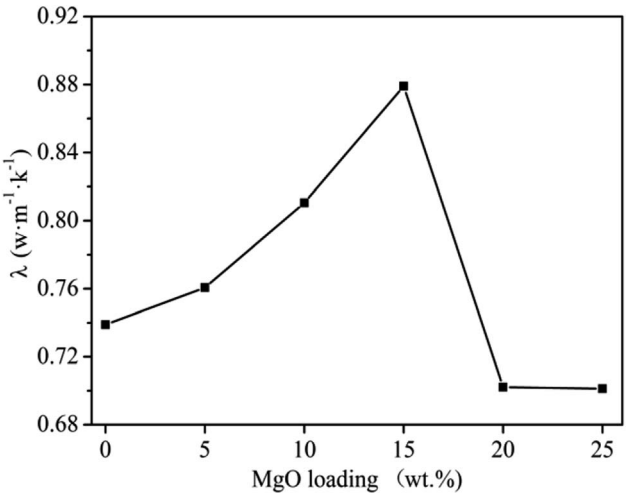

Fig. 5 Effect of MgO content on thermal conductivity of graphite/MgO/PVC at a milling speed of 150 r per min, milling time of 60 min and graphite contents of 20 wt%.

increasing MgO content could be attributed to several factors. Up to 15 wt% MgO contents filled the gaps between PVC molecules and hence formed a conductive network along-with graphite in PVC matrix.[11,12] This increases the heat conduction network and ultimately a higher thermal conductivity. Further increasing the MgO content (beyond 15 wt%) can envelop the conduction band and the network formed, which leads to a decrease in the thermal conductivity, as MgO has lower thermal conductivity than the network.[11] Therefore, an appropriate amount of MgO (15 wt%) is required for optimum thermal conductivity in graphite/MgO/PVC.

From the above results, one can conclude that optimum thermal conductivity of the graphite/MgO/PVC composites prepared in this study was achieved at a ball milling speed of 150 r per min, milling time of 60 min, and graphite and MgO contents of 15 wt% and 20 wt%, respectively. Furthermore, the thermal conductivity of graphite/MgO/PVC composite sheet at optimum conditions was 0.8791 W m^{-1} K^{-1} which was 6.27 times higher than that of pristine PVC and many reported PVC-based composites.[33,34]

3.5. SEM analysis of graphite/MgO/PVC composites

SEM images of the graphite/MgO/PVC composites (prepared by various techniques) and their fractured surfaces are shown in Fig. 6. As shown in Fig. 6a, pristine PVC was composed of concave and convex particles, which were rendered flatter by MA (Fig. 6b). This implied that MA destroyed the original structure of PVC which contributed to the uniform dispersion of fillers in the PVC matrix, greatly helping in the development of the conductive network and enhanced thermal properties of the composites. For comparison, graphite/MgO/PVC composites prepared by simple mixing were also analyzed by SEM (Fig. 6c) which suggested that a small amount of graphite and MgO were coated on the surface of PVC particles. As shown in Fig. 6d, under the combined effect of ball milling, shearing and friction during MA, graphite and MgO completely surrounded the PVC particles, which facilitated the formation of the thermal network throughout the PVC matrix. Furthermore, Fig. 6e and f showed that flake graphite was dispersed throughout the fracture of graphite/MgO/PVC composites prepared by simple mixing and exhibited a lower degree of cross-linking while the mesh structure of MgO was absent. On the contrary, the fractured surface of graphite/MgO/PVC composites prepared by MA (Fig. 6g and h) suggested a uniform dispersion of flake graphite in the PVC matrix and more obvious MgO links. These results confirmed the successful development of a thermal network in the graphite/MgO/PVC composites synthesized *via* MA, which greatly contributed to improving their thermal conductivity.

3.6. Thermal conductivity of composites

For a comparative analysis, the optimal thermal conductivity of the graphite/MgO/PVC composites was compared with that of the pristine PVC, graphite/PVC and MgO/PVC as depicted in Table 1 at optimal reaction conditions shown in Table 2. It can be seen from Table 1 that the MgO/PVC and graphite/PVC

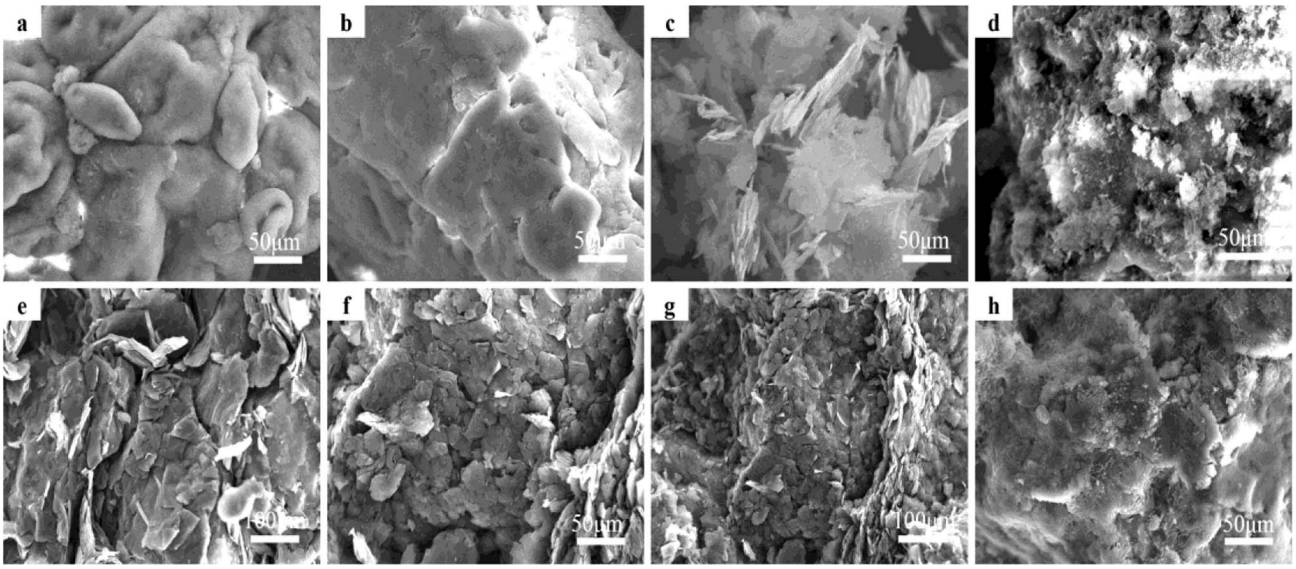

Fig. 6 SEM images of: (a) pristine PVC, (b) PVC treated by MA, (c) graphite/MgO/PVC composites prepared by simple mixing, (d) graphite/MgO/PVC composites prepared by MA, and (e) the fractured surface of graphite/MgO/PVC composites prepared by simple mixing and (f) by MA.

Table 1 Optimal thermal conductivity of different composites

Sample	Optimal thermal conductivity (W m^{-1} K^{-1})
Pristine PVC	0.1400
MgO/PVC	0.6734
Graphite/PVC	0.8394
Graphite/MgO/PVC	0.8791

composites prepared by MA ranked higher than that of the pristine PVC. This was attributed to the effective wrapping of MgO and graphite around PVC surface, high thermal properties of MgO and graphite, and high energy ball milling in MA, which collectively led to improved thermal conductivity.[2] Compared to pristine PVC, the MgO/PVC, graphite/PVC and graphite/MgO/PVC composites exhibited higher thermal conductivity (0.8791 W m^{-1} K^{-1}), which was attributed to the uniform wrapping of MgO and graphite around the surface of PVC by MA. Furthermore, MgO and graphite were believed to have integrated well in a synergistic mechanism in the PVC matrix, forming a thermal network in the PVC matrix and hence enhancing the thermal conductivity of the graphite/MgO/PVC composites. These results accord well with the SEM analysis (Fig. 6). Thus, graphite/MgO/PVC composites possessing higher thermal conductivity can be deemed as alternative candidates for practical applications, due to the simple and environmentally friendly synthesis approach and the low cost of graphite and MgO compared with metal based fillers.[2,3,11]

3.7. DSC analysis of composites

The glass transition temperature (Tg) data for pristine PVC, MgO/PVC, graphite/PVC and graphite/MgO/PVC composites determined by DSC are shown in Fig. 7. Fig. 7a suggests that the DSC curves of pristine PVC exhibited an exothermic peak at approximately 82.81 °C.[35] The Tg of MgO/PVC was 84.82 °C shown in Fig. 7b indicating that MgO with higher heat resistant and flame retardant properties could be wrapped around the surface of PVC by MA.[11,12] As seen from Fig. 7c, the Tg value (83.83 °C) for graphite/PVC partially improved compared with pristine PVC which was attributed to the high thermal conductivity and large surface area of graphite[3,8] and the high energy operation during MA.[22,23] Compared to pristine PVC, MgO/PVC and graphite/PVC, further increase in Tg *i.e.* 88.60 °C for graphite/MgO/PVC (Fig. 7d) was accredited to the encapsulation of graphite and MgO around PVC under MA. These results implied that the flame retardant MgO and highly thermally conductive graphite could be wrapped mutually in the PVC chain *via* MA approach, which enhanced the intermolecular forces and weakened the segmental mobility, resulting in an increased Tg for PVC.[9,35]

Table 2 Optimal reaction conditions of different composites preparation

Sample	MgO content (wt%)	Graphite content (wt%)	Milling speed (r per min)	Milling time (min)
MgO/PVC	30		150	50
Graphite/PVC		35	150	80
Graphite/MgO/PVC	20	15	150	60

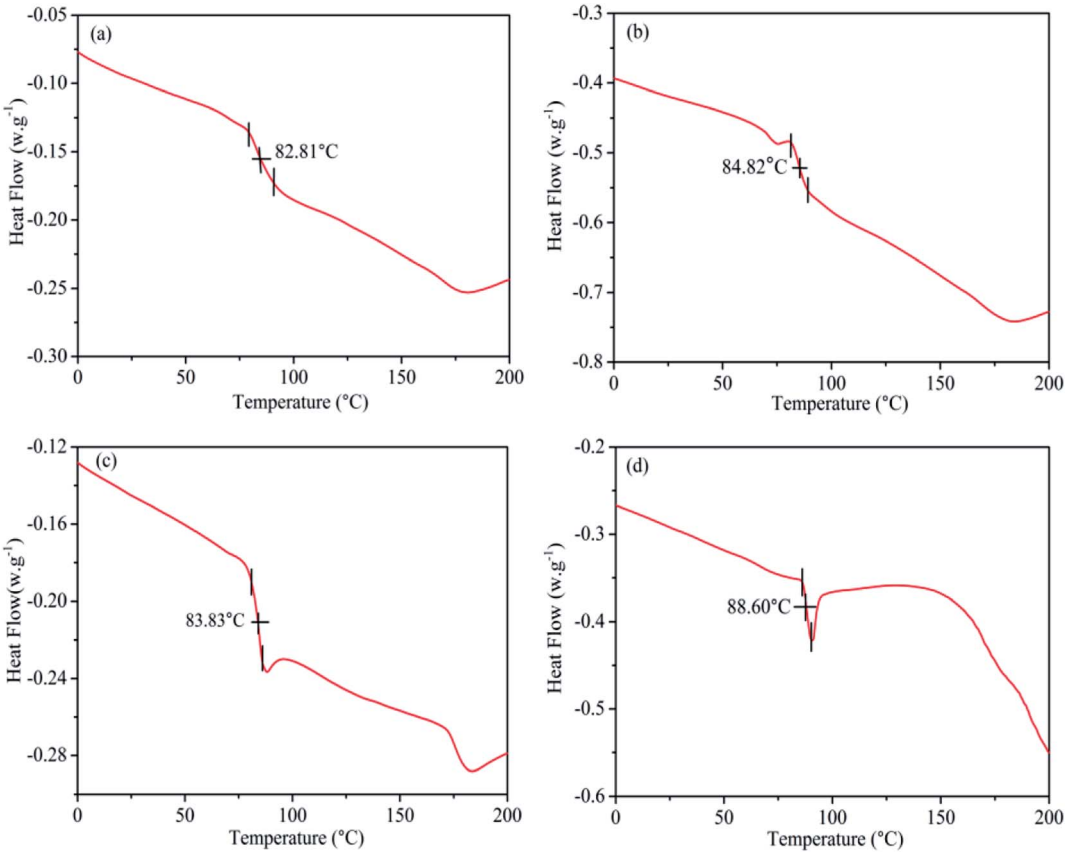

Fig. 7 DSC curves of: (a) pristine PVC, (b) MgO/PVC composite having 30 wt% MgO, (c) graphite/PVC composite having 35 wt% graphite and (d) graphite/MgO/PVC composite having 20 wt% graphite and 15 wt% MgO.

3.8. TGA and DTG analysis

TGA and DTG results of pristine PVC, MgO/PVC, graphite/PVC and graphite/MgO/PVC composites are depicted in Fig. 8. The TGA curves revealed two main degradation stages. The first weight loss occurred between 250–350 °C, which could be attributed to the loss of HCl originating from chlorine (Cl) radicals from the –C–Cl bonds and hydrogen radicals from the adjacent C–H groups.[36] The liberation of this HCl can lead to the formation of double bonds along the polymer chain.[37] The second decomposition was observed in the temperature range of 400–500 °C, which might be due to the degradation of the polyene backbones.[36] Furthermore, Fig. 8a suggests that the temperature at the maximum decomposition rate for pristine PVC was 287.61 °C,[38] which improved to 290.5 °C upon the incorporation of MgO in MgO/PVC (Fig. 8b) and can be attributed to the flame retardant and thermal stability of MgO[12] and the high-energy ball milling during MA.[22,23] Similarly, Fig. 8c suggests that TGA of graphite/PVC exhibits a higher degradation temperature (299.27 °C) than pristine PVC and MgO/PVC, implying that the thermally conductive graphite wrapped around the surface of PVC in the MA approach. Compared to pristine PVC, MgO/PVC and graphite/PVC, the decomposition temperature of graphite/MgO/PVC (Fig. 8d) was the highest (305.59 °C). This showed that highly flame retardant MgO and thermally conductive graphite could be wrapped mutually on the surface of PVC by MA and both MgO and graphite effectively hindered the decomposition of the chain segments, thereby increasing the thermal stability of PVC.[35,39,40]

3.9. Mechanical properties evaluation

Results of the tensile strength and bending strength tests of pristine PVC, MgO/PVC, graphite/PVC and graphite/MgO/PVC composites are presented in Fig. 9. As seen from Fig. 9a and b, the tensile strength and bending strength of pristine PVC were 60 MPa and 80 MPa, respectively, which after MgO incorporation (MgO/PVC) decreased to 48.73 MPa and 49.80 MPa, respectively. Similarly, the tensile strength and bending strength of graphite/PVC were 39.21 MPa and 53.21 MPa, respectively. Compared to MgO/PVC, the tensile strength of graphite/PVC was reduced, but the bending strength was improved due to its soft physical nature and superior ductility.[41] The tensile strength of graphite/MgO/PVC (47.39 MPa) was about 8 MPa higher than that of graphite/PVC, while its bending strength (51.98 MPa) was 2 MPa higher than that of MgO/PVC. This indicated that graphite and MgO had a synergistic effect under the high-energy ball milling in MA and played a key role in improving the mechanical properties of the final composites.

3.10. Mechanism of thermal enhancement by graphite/MgO/PVC composites

The proposed mechanism of thermal enhancement by graphite/MgO/PVC composites is illustrated in Fig. 10. The surface of

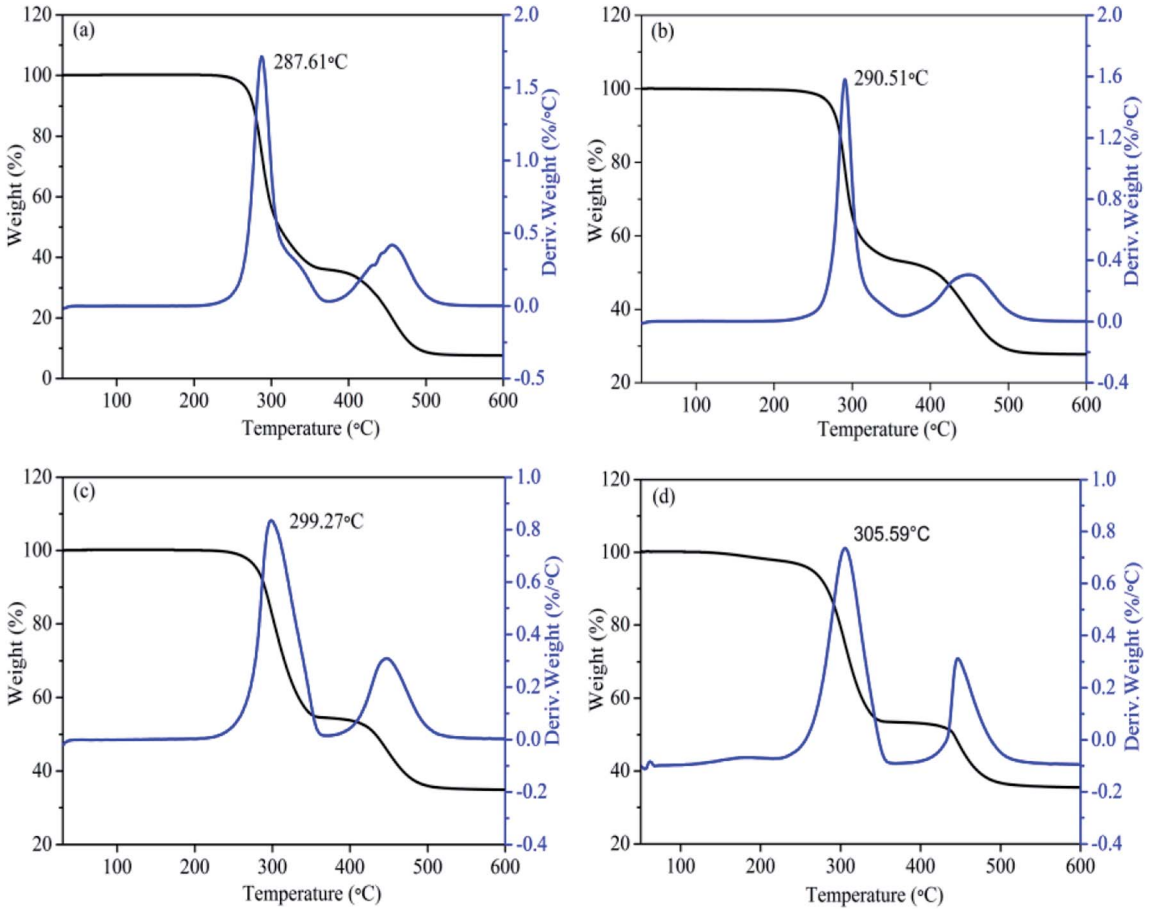

Fig. 8 TGA and DTG analysis of: (a) pristine PVC, (b) MgO/PVC composites having 30 wt% MgO, (c) graphite/PVC composites having 35 wt% graphite and (d) graphite/MgO/PVC composites having 20 wt% graphite and 15 wt% MgO.

pristine PVC was concave and convex, which after exposure to MA got flattened and hence could further affect the composite structure. Furthermore, in graphite/MgO/PVC, graphite and MgO were evenly wrapped on the surface of the PVC chains, which was in accordance with the SEM results (Fig. 6). In addition, due to the encapsulation of graphite and MgO, the thermal conductive network was efficiently formed in PVC matrix, concomitantly resulting in the enhancement of the Tg (Fig. 7d), the decomposition temperature (Fig. 8d) and the excellent mechanical properties (Fig. 9). From these results, one can conclude that the high thermal properties of graphite/MgO/PVC were mainly attributed to the uniform wrapping of graphite

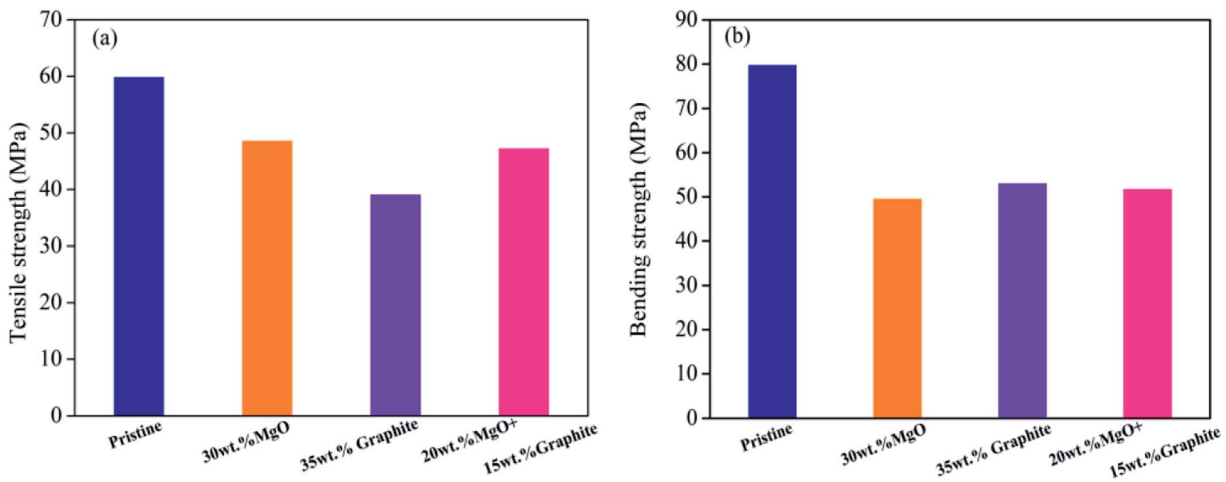

Fig. 9 (a) Tensile strength and (b) bending strength of different composites.

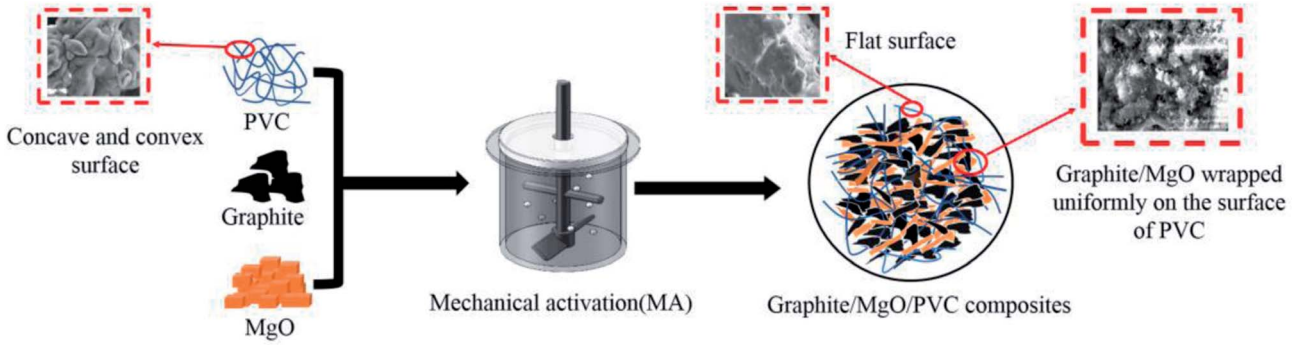

Fig. 10 Proposed mechanism of thermal enhancement by graphite/MgO/PVC composite.

and MgO in the PVC matrix, which was associated with the high thermal conductivity of graphite, high heat resistance of MgO and high-energy ball milling during MA.

4. Conclusions

In summary, graphite/MgO/PVC composites prepared by the MA approach showed uniform dispersion of graphite/MgO in the PVC matrix, which in turn led to enhanced thermal properties. Under optimum experimental conditions of 150 r per min ball milling speed, a milling time of 60 min, and graphite and MgO contents of 20 wt% and 15 wt% respectively, the thermal conductivity of pristine PVC was enhanced 6.27 times by graphite/MgO/PVC (0.8791 W m^{-1} K^{-1}). SEM results showed that flake graphite and MgO were uniformly dispersed in the PVC matrix and the thermal network was successfully formed in the graphite/MgO/PVC composites by MA, resulting in their enhanced thermal conductivity. DSC and TGA results, respectively, demonstrated that the Tg increased from 82.81 °C to 88.60 °C and there was a shift of 18 °C (from 287.61 °C to 305.59 °C) in the decomposition temperature for the graphite/MgO/PVC composites as compared to pristine PVC. These enhanced properties were attributed to the wrapping of high flame retardant MgO and high thermally conductive graphite around the surface of PVC by high-energy ball milling during MA. Compared to the pristine PVC, MgO/PVC and graphite/PVC, graphite/MgO/PVC exhibited enhanced bending strength and tensile strength. This study, due to the simplicity in operation, cost effectiveness and environmentally friendly nature of using MA, and in addition, the considerable enhancement of the thermal properties, could be deemed as an efficient alternative approach for the preparation of thermally resistant materials for practical applications on an industrial scale.

Conflicts of interest

There are no conflicts of interest to declare.

Acknowledgements

This research was supported by the Deans Project of Guangxi Key Laboratory of Petrochemical Resource Processing and Process Intensification Technology (No. 2017Z007), Youth project in Guangxi department of education (Grant No. 2018 KY0028), National Natural Science Foundation of China (No. 51463003), Guangxi Natural Science Foundation of China (No. 2017GXNSFEA198001 and 2016GXNSFAA380217), Guangxi Distinguished Experts Special Foundation of China, and the Scientific Research Foundation of Guangxi University (Grant No. XJPZ160713).

References

1 S. A. Mansour, M. E. Al-Ghoury, E. Shalaan, M. H. I. El Eraki and E. M. Abdel-Bary, *J. Appl. Polym. Sci.*, 2010, 3171–3177.
2 A. A. Al Ghamdi, F. Al Salamy, O. A. Al Hartomy, A. A. Al Ghamdi, A. M. Abdel Daiem and F. El Tantawy, *J. Appl. Polym. Sci.*, 2012, **124**, 1144–1153.
3 K. Kalaitzidou, H. Fukushima and L. T. Drzal, *Compos. Sci. Technol.*, 2007, **67**, 2045–2051.
4 S. Gabriel, R. W. Lau and C. Gabriel, *Phys. Med. Biol.*, 1996, **41**, 2271–2293.
5 G. Subodh, V. Deepu, P. Mohanan and M. T. Sebastian, *Polym. Eng. Sci.*, 2009, **49**, 1218–1224.
6 S. Liu, W. Yang, J. Lei and C. Zhou, *J. Appl. Polym. Sci.*, 2013, **127**, 3221–3227.
7 A. A. Al-Ghamdi and F. El-Tantawy, *Composites, Part A*, 2010, **41**, 1693–1701.
8 A. Yasmin and I. M. Daniel, *Polymer*, 2004, **45**, 8211–8219.
9 H. Quan, B. Zhang, Q. Zhao, R. K. K. Yuen and R. K. Y. Li, *Composites, Part A*, 2009, **40**, 1506–1513.
10 Z. Gao and L. Zhao, *Mater. Des.*, 2015, **66**, 176–182.
11 N. R. Dhineshbabu, P. Manivasakan, A. Karthik and V. Rajendran, *RSC Adv.*, 2014, **4**, 32161.
12 X. Li, K. Zhang, R. Shi, X. Ma, L. Tan, Q. Ji and Y. Xia, *Carbohydr. Polym.*, 2017, **176**, 246–256.
13 H. Wang, G. Xie, Z. Zhu, Z. Ying and Y. Zeng, *Composites, Part A*, 2014, **67**, 268–273.
14 K. Xu, K. Li, T. Zhong, L. Guan, C. Xie and S. Li, *Composites, Part B*, 2014, **58**, 392–399.
15 A. Kositchaiyong, V. Rosarpitak, B. Prapagdee and N. Sombatsompop, *Composites, Part B*, 2013, **53**, 25–35.
16 H. Wang, G. Xie, M. Fang, Z. Ying, Y. Tong and Y. Zeng, *Composites, Part B*, 2015, **79**, 444–450.
17 W. Zhou, C. Wang, T. Ai, K. Wu, F. Zhao and H. Gu, *Composites, Part A*, 2009, **40**, 830–836.

18 R. A. Hauser, J. A. King, R. M. Pagel and J. M. Keith, *J. Appl. Polym. Sci.*, 2008, **109**, 2145–2155.
19 J. Chen, X. Chen, F. Meng, D. Li, X. Tian, Z. Wang and Z. Zhou, *High Perform. Polym.*, 2016, **29**, 585–594.
20 F. He, H. Wu, X. Yang, K. Lam, J. Fan and L. H. Chan, *Polym. Test.*, 2015, **42**, 45–53.
21 O. Yousefzade, F. Hemmati, H. Garmabi and M. Mahdavi, *J. Vinyl Addit. Technol.*, 2016, **22**, 51–60.
22 Y. Zhang, T. Gan, Q. Li, J. Su, Y. Lin, Y. Wei, Z. Huang and M. Yang, *Appl. Surf. Sci.*, 2014, **314**, 603–609.
23 T. Gan, Y. Zhang, Y. Su, H. Hu, A. Huang, Z. Huang, D. Chen, M. Yang and J. Wu, *Cellulose*, 2017, **24**, 5371–5387.
24 Z. Liao, Z. Huang, H. Hu, Y. Zhang and Y. Tan, *Bioresour. Technol.*, 2011, **102**, 7953–7958.
25 W. Wang, W. Zhang, S. Zhang and J. Li, *Constr. Build. Mater.*, 2014, **65**, 151–158.
26 L. Deris, S. Sharafi and G. H. Akbari, *J. Therm. Anal. Calorim.*, 2014, **115**, 401–407.
27 H. Hu, W. Liu, J. Shi, Z. Huang, Y. Zhang, A. Huang, M. Yang, X. Qin and F. Shen, *Starch-Starke*, 2016, **68**, 151–159.
28 I. Bonadies, M. Avella, R. Avolio, C. Carfagna, G. Gentile, B. Immirzi and M. E. Errico, *Polym. Test.*, 2012, **31**, 176–181.
29 Q. Zhou, C. Tang, Y. Wang and L. Zheng, *Fuel*, 2004, **83**, 1727–1732.
30 S. M. Grimes, H. Lateef, A. J. Jafari and L. Mehta, *Polym. Degrad. Stab.*, 2006, **91**, 3274–3280.
31 H. Hu, Y. Zhang, X. Liu, Z. Huang, Y. Chen, M. Yang, X. Qin and Z. Feng, *Polym. Bull.*, 2014, **71**, 453–464.
32 I. L. Ngo, C. Byon and B. J. Lee, *Int. J. Heat Mass Transfer*, 2018, **126**, 474–484.
33 S. A. Mansour, M. Hussein and A. H. Moharram, *Adv. Polym. Technol.*, 2014, **33**, 21431–21439.
34 R. D. Maksimov, J. Zicans, T. Ivanova, S. N. Negreeva and E. Plume, *Mech. Compos. Mater.*, 2002, **38**, 141–148.
35 P. Jia, L. Hu, G. Feng, C. Bo, M. Zhang and Y. Zhou, *Mater. Chem. Phys.*, 2017, **190**, 25–30.
36 F. Ma, N. Yuan and J. Ding, *J. Appl. Polym. Sci.*, 2013, **128**, 3870–3875.
37 K. Deshmukh and G. M. Joshi, *Polym. Test.*, 2014, **34**, 211–219.
38 S. S. Suresh, S. Mohanty and S. K. Nayak, *J. Polym. Res.*, 2017, **24**, 120.
39 P. Jia, M. Zhang, C. Liu, L. Hu, G. Feng, C. Bo and Y. Zhou, *RSC Adv.*, 2015, **5**, 41169–41178.
40 P. Jia, M. Zhang, L. Hu, C. Liu, G. Feng, X. Yang, C. Bo and Y. Zhou, *RSC Adv.*, 2015, **5**, 76392–76764.
41 T. Andriollo, S. Fæster and G. Winther, *Mech. Mater.*, 2018, **122**, 85–95.